Military Technical College
Kobry El-Kobbah,
Cairo, Egypt

6th International Conference
on Electrical Engineering
ICEENG 2008

An experimental model of fuel cell/microturbine generation scheme

By

M. Soliman * M. Safiuddin **

Abstract:

In this paper a dynamic and steady state model of a distributed generation scheme is presented. Both the dynamic and steady state results of the simulation model are verified with those obtained from a laboratory prototype and the results showed a close agreement. The experimental model was designed to supply isolated loads as well as in parallel with the grid.

The proposed system consists of a microturbine driving a Permanent Magnet Synchronous Generator (PMSG). The ac power generated from the PMSG is rectified and, along with a Fuel Cell, is connected to the dc-link. A PWM inverter delivers ac power to the load.

The laboratory prototype uses a dc motor as the prime mover for a separately excited dc generator representing the fuel cell, while the microturbine is modeled using a shunt dc motor as the prime mover for a three phase PMSG.

Keywords:

Distributed Generation, Microturbine, Modulation index, Permanent Magnet Synchronous Generator (PMSG), Pulse Width Modulation, Solid Oxide Fuel Cell (SOFC).

* Department of Electrical /Electronics Technology at the University College of the North, Thompson, MB, Canada (e-mail: msoliman@ucn.ca)

** Department of Electrical Engineering, State university of NY at Buffalo, Buffalo, NY, USA (e-mail: safium@eng.buffalo.edu).

1. Introduction:

THE demand for energy is ever increasing globally and the efficient usage of energy has become an important issue all over the world. According to the International Energy Agency (IEA), an estimated $16 trillion will be needed as capital investment in world's energy systems over the next 25 years to meet this growing demand.

Fuel Cells are a rapidly developing power conversion technology for both central and distributed electrical power generation. As compared to micro-turbines and Internal Combustion (IC) engines, fuel cells offer relatively high conversion efficiencies with respect to fuel input, low emissions, low noise operation, and high reliability. Power is produced by the electrochemical reaction that results from passing a hydrogen rich gas over an electrode called the anode and air over the other electrode, the cathode. The exchange of ions between the electrodes is facilitated by the electrolyte.

Work has been reported in the literature on steady state modeling [1], [2], and on dynamic modeling [3] - [7] of fuel cells. Fuel cells seem to be a good choice for distributed generation. The Solid Oxide Fuel Cell (SOFC) has the following promising characteristics: 1) the by-product is water; 2) High temperature operation, which allows it to be integrated into Combined Heat and Power (CHP) systems, and 3) it uses a solid polymer as an electrolyte, which is safer in manufacturing, operation and maintenance.

The motivation behind the idea of this paper comes from research on application of a fuel cell combined with another Distributed Generation (DG) source for peak power shaving [8]. Because of the high cost involved in the fuel cells, it was difficult to verify the results obtained from computer simulations. It also makes it difficult to develop small-scale experimental models with limited funds. On the other hand, the reduced cost and flexibility of the fuel cell emulators provide a good training module for students and application engineers.

Fuel cells are classified according to the heat generated from the chemical reaction into low temperature fuel cells like Proton Exchange Membrane Fuel Cells (PEMFC) operating in the range of 100 ^{o}C; medium temperature fuel cells like Phosphoric Acid Fuel Cells (PAFC); and high temperature fuel cells like Molten Carbonate Fuel Cells (MCFC) and Solid Oxide Fuel Cells (SOFC), where the temperatures generated are between 650-1100 ^{o}C.

Different simulators of the fuel cell have been proposed and reported in the literature [2, 9-12]. They vary between simulating the steady state or the dynamic response of the FC. These models use the controlled rectifier to represent the fuel cell dynamics.

In order to build a good fuel cell simulator, a reliable mathematical model of the fuel cell is first developed, which allows the evaluation of the fuel cell dynamic response as well as its steady state performance. The dynamic response of the generating system is important from the control and system management points of view.

When considering CHP applications, the microturbine/ fuel cell scheme has higher overall efficiency compared to other cogeneration schemes. Low emission is another benefit from using the proposed scheme.

In this paper, section 2 describes the proposed scheme and the derivation of the mathematical model, section 3 illustrates the experimental model, section 4 gives the results from both simulation and the experimental model, and conclusions are presented in section 5.

2. System description

The proposed system shown in Figure (1) consists of a single shaft microturbine driving a permanent magnet synchronous generator, which produces ac power with variable frequency depending on the rotor speed of the generator. Because of the variable frequency nature of the generated voltage, a three-phase full wave bridge rectifier is used to rectify the ac power into dc at the dc-link. A Solid Oxide Fuel Cell (SOFC) is also connected to the dc-link. Since most loads require AC supply, the dc power is inverted into ac at the load side by use of a PWM inverter. A transformer connects the inverter to the load. Although this system is modeled and tested for isolated loads it can be used to supply grid-connected loads as well.

A. Microturbine

A large body of literature on modeling of microturbines has been reported [13]- [17]. Since the torque required from the microturbine is the only mechanical variable of interest rather than the mechanical behavior of the microturbine, the simplified model in Figure (2) is used to represent the microturbine [14], [17].

Fig. 1. The proposed peak power shaver comprising a microturbine driving a PMSG, connected to a 3-phase full wave diode bridge rectifier. A SOFC is connected to the dc-link. A PWM inverter conditions the dc power into ac for the load.

Fig. 2. A simplified model of the microturbine.

The microturbine consists of two parts, the mechanical prime mover and the electrical generator. The model for the mechanical part is divided into two subsystems, the fuel system and the turbine. The fuel system consists of the fuel valve and actuator. For a fuel signal (F_d) into the fuel system, the valve positioner equation is [17]:

$$e_{FC} = \frac{a}{bs + c} F_d \tag{1}$$

Where the constants a, b and c are taken from [15]. Feeding the actuator by the signal (e_{FC}), its output is:

$$w_{FC} = \frac{k_{fc}}{\tau_{fc} s + 1} e_{FC} \tag{2}$$

Where k_{fc} and τ_{fc} are actuator gain and time constant, respectively.
The microturbine torque equation is:

$$T = 1.3(w_{FC} - 0.23) + 0.5(\Delta\omega) \tag{3}$$

The torque speed relation of the microturbine is shown in Figure (3), where it can be approximated into a second order relation as:

$$T = -7.7 N \omega_e^2 + 7.2\omega_e + 0.5 \quad \text{pu} \tag{4}$$

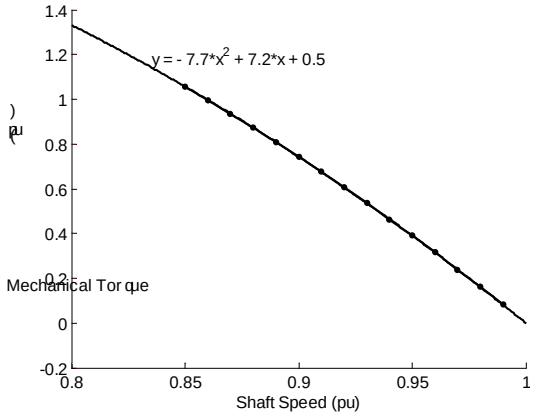

Fig. 3. The steady state relation between the microturbine torque and shaft speed.

The electrical generator used is of the PMSG type. The dynamic equations of the generator represented in the d-q axes are [18]:

$$v_{qs} = -R_s i_{qs} + L_{qs} P i_{qs} - \omega_e L_{ds} i_{ds} + \omega_e \lambda_F \tag{5}$$

$$v_{ds} = -R_s i_{ds} + L_{ds} P i_{ds} - \omega_e L_{qs} i_{qs} \tag{6}$$

Using the rotor reference frame and assuming the generator phase voltage to be aligned with the q- axis, we get the following relationships:

$$v_{qs} = V_s \quad (7)$$

$$v_{ds} = 0 \quad (8)$$

Where, V_s is the peak value of the generator stator voltage.

B. Bridge Rectifier

A three-phase diode bridge rectifier is used to convert the ac output of the PMSG to dc at the dc-link. The average value of the rectifier output voltage (V_{DC}) can be expressed in terms of the peak of the generator phase voltage as:

$$V_{DC} = \frac{3\sqrt{3}}{\pi} v_{qs} \quad (9)$$

Assuming the rectifier to be lossless, the instantaneous real power on the ac side must equal that on the dc side, that is,

$$V_{DC} I_{DC} = \frac{3}{2} v_{qs} i_{qs} \quad (10)$$

Substituting the value of (V_{DC}) from (9) into (10), the rectifier current is

$$I_{DC} = \frac{\pi}{2\sqrt{3}} i_{qs} \quad (11)$$

As an uncontrolled rectifier is being used, no reactive power will be transferred from the PMSG to the dc link and hence the value of i_{ds} will be zero.

In order to write the differential equations for the overall system, we need to transform the electrical quantities from the dc side of the rectifier to the generator side. Using (9) and (11) the transformations are:

For resistance and inductance:

$$Z^{g} = \frac{\pi^{2}}{18} Z \quad (12)$$

Voltage transformation:

$$V_{DC}^{g} = \frac{\pi}{3\sqrt{3}} V_{DC} \quad (13)$$

Current transformation:

$$I_{DC}^{g} = \frac{2\sqrt{3}}{\pi} I_{DC} \quad (14)$$

Where the superscript g represents the quantity referred to the generator side and Z represents resistance and/or inductance.

C. Fuel Cell Model

Fuel cells convert the chemical energy contained in a fuel into electrical energy as

illustrated in Figure (4) [19]. The chemical reactions directly involved in the production of electricity are given by:

At the anode:

$$H_2 + O^{=} \rightarrow H_2O + 2e^{-}$$

At the cathode:

$$O_2 + 4e^{-} \rightarrow 2O^{=}$$

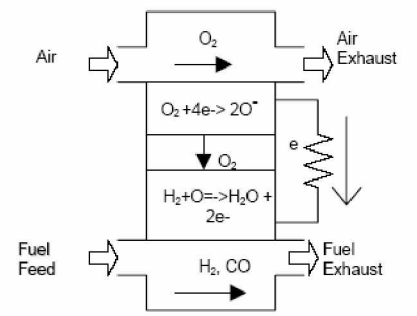

Fig. 4. Solid Oxide Fuel Cell (SOFC) basic operation.

The developed model was based on the following assumptions:

- The fuel used is pure hydrogen; the fuel reformer is not modeled.
- Cell temperature is constant. Temperature variations across the stack are neglected, and the heat capacity of the cell is assumed constant.
- Only activation and ohmic losses are considered, by keeping the ratio of fuel to air constant all the time the effect of the concentration overvoltage can be ignored.

The mathematical model of the fuel cell is derived by calculating the change in partial pressures of different reaction components, given by [7]:

$$\frac{dp_{H_2}}{dt} = \frac{1}{\tau_{H_2}}[\frac{1}{k_{H_2}}(q_{H_2}^{in} - 2K_r i_{fc}) - p_{H_2}] \quad (15)$$

$$\frac{dp_{O_2}}{dt} = \frac{1}{\tau_{O_2}}[\frac{1}{k_{O_2}}(q_{O_2}^{in} - K_r i_{fc}) - p_{O_2}] \quad (16)$$

$$\frac{dp_{H_2O}}{dt} = \frac{1}{\tau_{H_2O}}[\frac{1}{k_{H_2O}} 2K_r i_{fc} - p_{H_2O}] \quad (17)$$

The ratio of the molar flow rate of oxygen and that of hydrogen is kept constant at 0.856. The above equations describe three decoupled first order linear differential equations with inputs the inlet molar flow of hydrogen and the fuel cell output current. The above equations can be solved to give:

$$p_{H_2} = (1 - e^{\frac{-t}{\tau_{H_2}}})(\frac{q_{H_2}^{in} - 2K_r i_{fc}}{k_{H_2}}) \quad (18)$$

$$p_{O_2} = (1 - e^{\frac{-t}{\tau_{O_2}}})(\frac{q_{O_2}^{in} - K_r i_{fc}}{k_{O_2}}) \quad (19)$$

$$p_{H_2O} = (1 - e^{\frac{-t}{\tau_{H_2O}}})(\frac{2K_r i_{fc}}{k_{H_2O}}) \quad (20)$$

The output voltage from the fuel cell is calculated by using the Tafel equation as,

$$V_{fc} = E_{fc} - V_{ohmic} - V_{activation} - V_{concentrat\ ion}. \quad (21)$$

The value of the Nernst Voltage (E_{fc}) is found from Nernst Equation:

$$E_{fc} = N_0\left(E_0 + \frac{RT}{2F}\left[\ln\frac{p_{H_2} p_{O_2}^{1/2}}{p_{H_2O}}\right]\right) \quad (22)$$

The ohmic overvoltage (V_{ohmic}) is due to electrical resistance of electrodes and the resistance to the flow of ions in the electrolyte [12] and is calculated by ohm's law.

$$V_{ohmic} = i_{fc} * R_{fc}$$

The activation overvoltage ($V_{activation}$) is a function of the cell current and hydrogen concentration [3]. It can be represented by the following equation.

$$V_{activation} = B \ln C\, i_{fc}$$

Where, the constants B and C depend on the cell type.

By assuming that the fuel cell is operating in the linear region and that the flow of hydrogen and oxygen is kept constant, the concentration overvoltage ($V_{concentrat\ ion}$) is ignored in deriving the model [7]. The block diagram representing the fuel cell model is shown in Figure (5).

D. Pulse Width Modulated Inverter

Fourier analysis of the output voltage from the inverter takes the following form [20]:

$$v_i = m\frac{V_R}{2}\sin(\omega t + \delta) + \text{Besselterms} \quad (23)$$

Ignoring the higher frequencies, the amplitude of the inverter output voltage in a synchronously rotating reference frame can be expressed as;

$$v_{qinv} = m\frac{V_R}{2} \quad (24)$$

Where, the quadrature axis is assumed to align with v_{qinv}.

Fig. 5. SOFC fuel cell model, the inputs to the model are i_{fc} which is determined from the electrical circuit connected to the fuel cell and ($q_{H_2}^{in}$) from the fuel reformer.

Assuming the inverter to be lossless, the instantaneous real power from the inverter is equal to the dc link power, that is

$$\frac{3}{2} v_{qinv} i_{qinv} = v_{dc} i_{dc};$$

From which the inverter output current is related to the dc link current by:

$$i_{qinv} = \frac{4}{3m} i_{dc} \tag{25}$$

Referring the ac side quantities of the inverter to the dc-link side by using (24) and (25) we get:

$$v_{qinv}^{DC} = \frac{2}{m} v_{qinv} \tag{26}$$

and ,

$$i_{qinv}^{DC} = \frac{3m}{4} i_{qinv} \tag{27}$$

Where, the superscript *DC* refers to the *dc* link side of the inverter.

E. Overall System Model

After referring all quantities into the PMSG side the overall system equations can be written from the equivalent circuit shown in Figure (6) as:

$$Pi_{qs} = \frac{1}{L_{qs} + L_r^g} [\lambda_F \omega_e + R_{fc}^g i_i^g - \mathrm{E}_{\mathrm{fc}}^{\mathrm{g}} - (R_s + R_r^g + R_{fc}^g) i_{qs}] \tag{28}$$

$$Pi_i^g = \frac{1}{L_i^g + L_l^g} [E_{fc}^g + R_{fc}^g i_{qs}^g - (R_i^g + R_l^g + R_{fc}^g) i_i^g] \tag{29}$$

And the mechanical equations

$$T_e = \frac{3p}{4} (\lambda_F i_{qs} + (L_{ds} - L_{qs})(i_{qs} i_{ds})) \tag{30}$$

$$P\omega_e = \frac{p}{2}\frac{1}{J}[T_m - T_e - B\omega_e] \quad (31)$$

Fig. 6. q-axis equivalent circuit for PPS.

3. Emulation model

a) *Fuel Cell*

The proposed model consists of a separately excited dc generator. The output voltage from the dc generator is controlled by controlling its field current. Using a fully controlled single-phase bridge rectifier, the generator's field current can be changed in order to control its output voltage. Because of the nearly constant speed versus torque characteristics of the shunt motor, it is used to drive the dc generator at constant speed. The large inductance in the generator field circuit does not allow it to generate when supplied directly from the rectifier. To solve this problem, a capacitor bank is placed on the output of the rectifier and is used to reduce the fluctuations in the rectifier's output voltage, as shown in the block diagram [Figure (7)].

The control algorithm followed to present the fuel cell characteristics is as follows. By measuring the load current, the controller calculates the corresponding fuel cell voltage (E_{fc}) from equations (18-22). The difference between the fuel cell voltage (E_{fc}) and the generator's output voltage (V_g) goes into a PI controller which controls the firing instants of the rectifier and hence the value of the generator's output voltage.

Because the proposed model is a laboratory small scale size and is intended to represent small size as well as large size fuel cells, per unit values are used to represent different electrical quantities where the base values of which are included in the control program. These base quantities can be changed in the control program to represent different fuel cells.

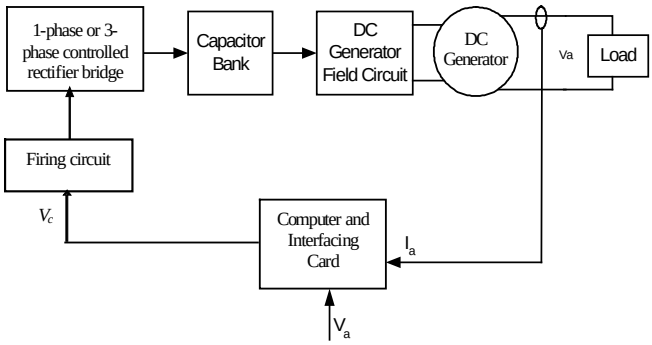

Fig. 7. Block diagram of the fuel cell emulation model.

Figure (8) shows a photograph of the laboratory setup. Using a data interface card, the measured signals from the generator terminals are conditioned into a range suitable for the Data Acquisition Card (DAQ). An NI-6025E DAQ is used to read the signals and generate the rectifier control voltage. The software used is LabView because of its advanced capabilities to do real time measurements and control. The Graphic User Interface (GUI) of the software allows the user to change different fuel cell parameters in real time and notice the changes it has on the model.

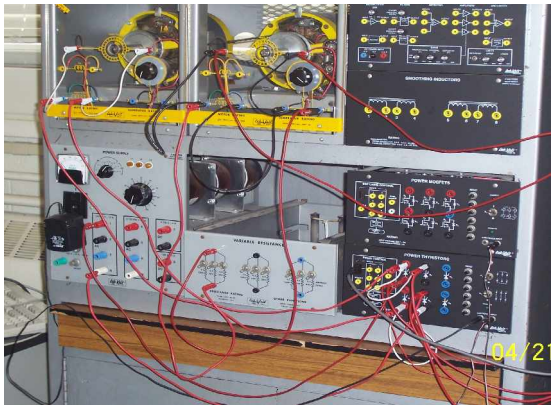

Fig. 8. Emulation model of SOFC using a shunt dc motor driving a separately excited dc generator representing the fuel cell. The drive motor armature voltage represents the FC hydrogen flow.

b) Microturbine

The steady state characteristics of the mechanical part of the microturbine are represented using a shunt dc motor which drives the PMSG. Following Equation (1) the torque produced from the Microturbine at any instant can be estimated by knowing the corresponding per unit value of the shaft speed. Figure (9) shows a block diagram of the laboratory model of the microturbine. Two signals are measured from the shunt motor its rotor speed (N_r) and its armature current (I_a). The difference between the armature current and the calculated armature current is fed into a PI controller which determines

the control voltage to the single-phase rectifier.

Fig. 9. Block diagram of microturbine emulation model.

4. Simulation and experimental results

The proposed model was simulated using MatLab and the simulation results are shown in Figures (10-15). During these simulations the load changed from 0.47 to 0.65 pu at 75 sec. and was then removed at 370 sec. Load insertion and rejection is shown in Figure (10). The load current is shared between the fuel cell and microturbine which is shown in Figures (11), (13). Due to the increase in the fuel cell current, the fuel cell voltage is reduced as shown in Figure (12). In order to keep the output load voltage constant, the value of the modulation index is controlled using a PI controller as shown in Figure (14). Figure (15) shows the load real power output from the system.

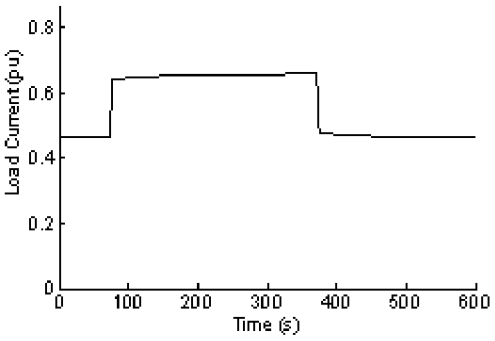

Fig. 10. Load current a step increase in the load is applied to the system at t=75 sec and then removed at t=370 sec.

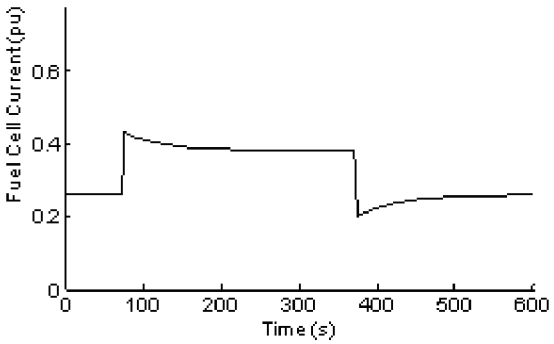

Fig. 11. Change in the fuel cell current due to step change in the load.

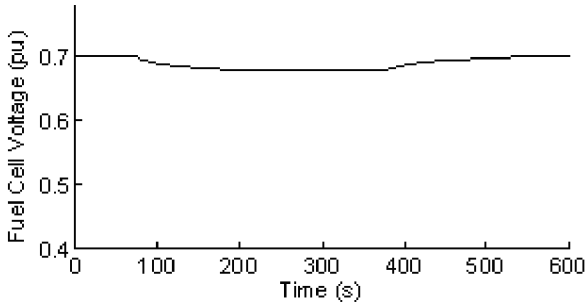

Fig. 12. Fuel cell voltage.

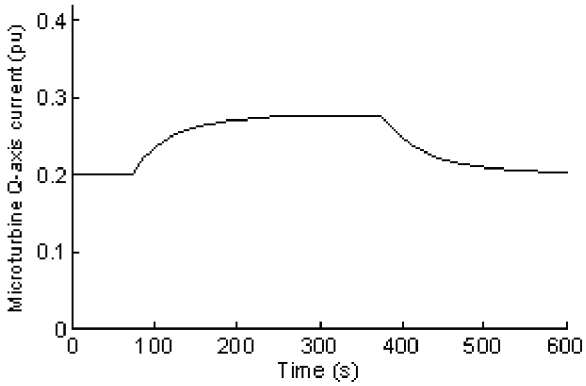

Fig. 13. Microturbine q-axis current.

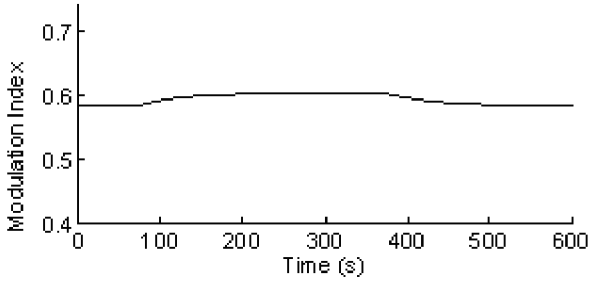

Fig. 14. PWM inverter modulation index.

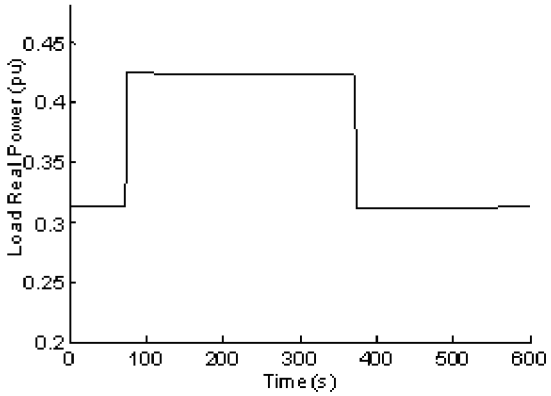

Fig. 15. Load real power.

The experimental model is used to verify the simulation results presented above and the results are shown in Figures (16)-(21). During the experiment the load voltage was kept constant at 1 pu. Comparison between the experimental measurements and the corresponding simulation results shows a close agreement for all the curves except for the microturbine current in Figures (17) and (13), the reason for this is that, only the steady state torque-speed relation of the microturbine is modeled in the system. Figure (16) shows the load current where the load is increased at 70 sec and removed at 240 sec. Figure (17) shows the microturbine current. Fuel cell current is illustrated in Figure (18) a small overshoot occurs in the fuel cell current and is limited by the inductance associated with the generator armature inductance. The generated voltage corresponding to the fuel cell current is shown in Figure (19). Figure (20) shows the change in modulation index in order to get the required load voltage and the corresponding load real power shown in Figure (21).

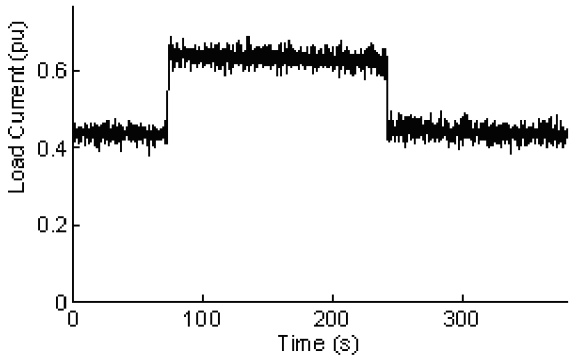

Fig. 16. Experimental load current.

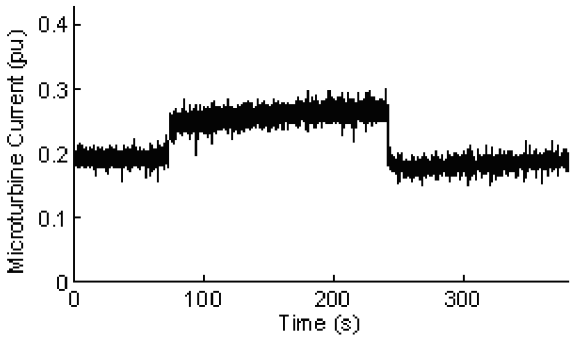

Fig. 17 Microturbine current.

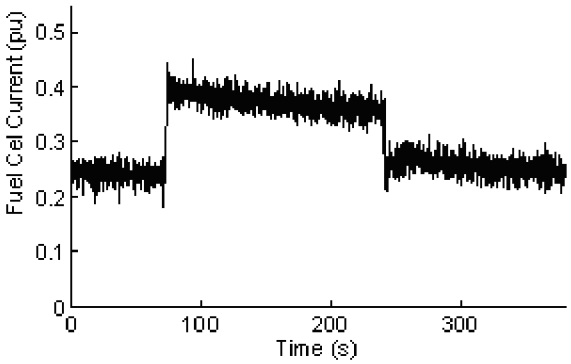

Fig. 18. Fuel Cell current.

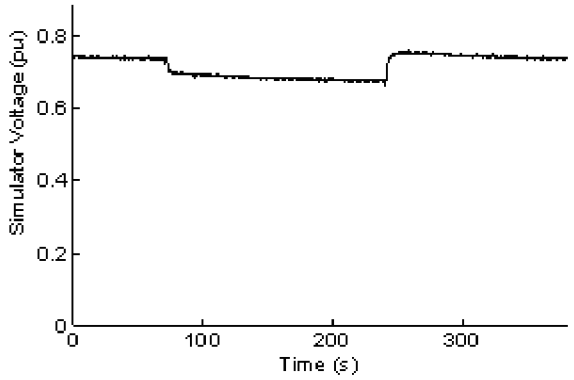

Fig. 19. Simulator output voltage.

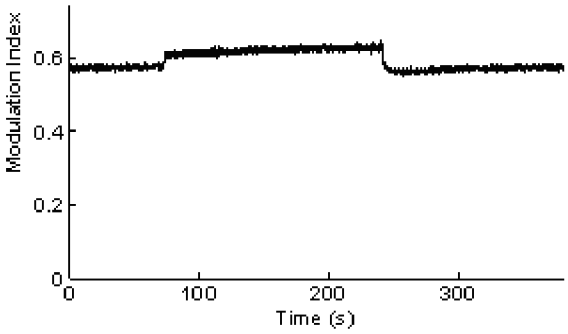

Fig. 20. PWM inverter modulation index.

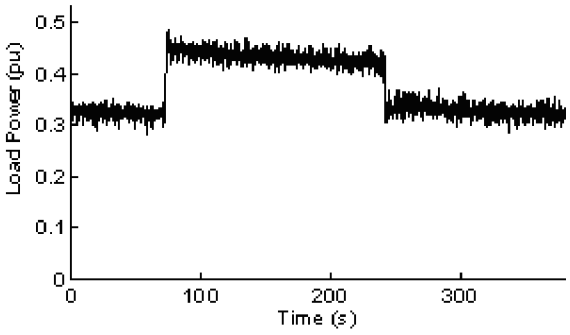

Fig. 21. Load Power.

5. Conclusion

In this paper, a distributed generation scheme has been presented. The mathematical dynamic model has been derived. A laboratory model was built to produce the characteristics of the computer model. The experimental results confirmed a close agreement with computer simulations. This study showed that a separately excited dc generator can be used to represent a fuel cell. The high inductance in the generator's field circuit allows it to simulate the slow fuel cell dynamics. This model has been designed to supply isolated loads as well as those connected to the power grid. It can

also be integrated with different distributed generation sources for peak power shaving of connected loads.

Acknowledgment

The authors thank Dr. Ilya Grinberg of Buffalo State College, State University of New York, Buffalo, NY., for his assistance offering the lab facilities and equipment for the experimental part of the research and development work.

References:

[1] R. F. Mann, et al., *Development and Application of a Generalized Steady State Electrochemical Model for a PEM Fuel Cell*, Journal of Power Sources, Vol. 86, 2000, pp. 173-180.

[2] P. Acharya, P. Enjeti and I. J. Pital, *An Advanced Fuel Cell Simulator*, IEEE APEC 04 19th annual Applied Power Electronics Conference and Exposition, 2004, Vol. 3, pp. 1554-1558.

[3] M. Y. El-Sharkh, et al., *Analysis of Active and Reactive Power Control of a Stand Alone PEM Fuel Cell Power Plant*, IEEE Transactions on Power Systems, Vol. 19, No. 4, November 2004, pp. 2022-2028.

[4] J. M. Correa, et al., *An Electrochemical Based Fuel Cell Model Suitable for Electrical Engineering Automation Approach*, IEEE Transactions on Industrial Electronics, Vol. 51, No. 5, October 2004, pp. 1103-1111.

[5] C. J. Hatziadoniu, A. A. Lobo, F. Pourboghrat and M. Daneshdoost , *A Simplified Dynamic Model of Grid Connected Fuel Cell Generators*, IEEE Transactions on Power Delivery, Vol. 17, No. 2, April 2002, pp. 467-473.

[6] C. Wang, H. Nehrir and S. R. Shaw, *Dynamic Model and Model Validation for PEM Fuel Cells Using Electrical Circuits*, IEEE Transactions on Energy Conversion, Vol. 20, No.2, June 2005, pp. 442-451.

[7] J. Padulles, G. W. Aulr and J. R. McDonald, *An Integrated SOFC Plant Dynamic Model for Power Systems Simulation*, Journal of Power Sources, 86, 2000, pp. 495-500.

[8] M. Soliman, A. Puppala and M. Safiuddin, *Dynamic Analysis of Microturbine/ Fuel Cell for Peak Power Shaving*, IEEE-PES General Meeting, June 18-22, 2006.

[9] J. M. Correa F. A. Farret, J. R. Gomes and M. G. Simoes, *Simulation of Fuel Cell Stacks Using a Computer-Controlled Power Rectifier With the Purpose of Actual High-Power Injection Applications*, IEEE Transactions on Industry Applications, Vol.39, N0. 4, July/August 2003, pp. 1136-1142.

[10] N-A. Parker, A. T. Bryant and B. R. Palmer, *The Application of Fuel Cell Emulation in the Design of an Electric Vehicle Powertrain*, IEEE 36th Conference on Power Electronics Specialists, June 12, 2005, pp. 1869-1874.

[11] T. W. Lee, et al., *A 3 Kw Fuel Cell Generation System Using the Fuel Cell Simulator*, IEEE Int'l Symposium on Industrial Electronics, Vol. 2, May 2004, pp.833-837.

[12] M. Ordonez, M. T. Iqbal and J. E. Quaicoe, *Development of a Fuel Cell Simulator Based on an Experimentally Derived Model*, Canadian Conference on Electrical and Computer Engineering, May 1-4, 2005, pp. 1457-1460.

[13] R. Lasseter, *Dynamic Models for Microturbines and Fuel Cells*, IEEE Power Engineering Society Summer Meeting, Vol. 2, July 2001, pp. 761-766.

[14] W. I. Rowen, *Simplified Mathematical Representations of Heavy-Duty Gas Turbines*, Transactions of the ASME Journal of Engineering for Power, Vol. 105, Oct 1983, pp. 865-869.

[15] L. M. Hajagos and G. R. Berube, *Utility Experience with Gas Turbine Testing and Modeling*, IEEE Transactions on Power Systems, Vol.13, No.1, Feb.1998, pp.165 – 170.

[16] M. Etezadi-Amoli and K. Choma, *Electrical Performance Characteristics of a New Micro-Turbine Generator*, IEEE Power Engineering Society Winter Meeting, Vol. 2, 2001, pp.736 – 740.

[17] A. Cano and F. Jurado, *Modeling Micro-Turbines on the Distribution System Using Identification Algorithms*, Proceedings of IEEE Conference on Emerging Technologies and Factory Automation

(ETFA), Vol. 2, 16-19 Sept. 2003, pp.717 – 723.
[18] R. H. park, *Two-Reaction Theory of Synchronous Machines- Generalized Method of Analysis-Part I*, AIEE Transactions, Vol. 48, July 1929, pp. 716-727.
[19] K. Sedghisigarchi and A. Feliachi, *Control of Grid Connected Fuel Cell Power Plant for Transient Stability Enhancement*", *IEEE Power Engineering Society winter meeting, Vol. 1, 27-31 Jan. 2002, pp. 383-388.*
[20] B. K. Bose, *Power Electronics and AC Drives*, Prentice-Hall, Englewood Cliffs, NJ, 1986.

Nomenclatures:

E_0	Open cell voltage (V).
E_{fc}	Fuel Cell emf.
F	Faraday's constant (C/kmol).
$K_r = \frac{N_0}{4F}$	Modeling constant (kmol/sA).
I_{DC}	Dc- link current (A).
J	Rotor inertia.
L_r, L_i	The rectifier and inverter inductance, respectively.
L_{qs}, L_{ds}	Stator quadrature and direct axis inductances, respectively.
N_0	Number of cells in series in the stack.
P	Number of poles of the PMSG.
R	Universal gas constant (J K/kmol).
R_{fc}	Fuel cell electrical resistance.
R_l	Load resistance (Ω)
R_r	Rectifier resistance (Ω)
R_s	Rotor resistance (Ω).
T	Stack temperature (K).
T_e	Electromagnetic torque from the PMSG
T_m	Mechanical torque generated from the microturbine
V_{DC}	dc link voltage.
i_{fc}	Fuel cell current. (A).
i_i^g	Inverter output current referred to generator side.
i_{ds}, i_{qs}	PMSG 's direct-, quadrature- axis currents, respectively.
$k_{H_2}, k_{O_2}, k_{H_2O}$	Fuel, air and fuel exhaust valves molar constant, respectively (kmol/atm s).
m	The inverter modulation index.
$p_{H_2}, p_{O_2}, p_{H_2O}$	Partial pressure of hydrogen, oxygen and water respectively (atm).
$q_{H_2}^{in}, q_{O_2}^{in}$	Inlet molar flow of hydrogen and oxygen (kmol/s).
v_{ds}, v_{qs}	Generator's quadrature, direct axis voltage, respectively.
δ	Phase shift of the output waveform.
λ_F	Permanent magnet flux linkage amplitude.
$\tau_{H_2}, \tau_{O_2}, \tau_{H_2O}$	Fuel, air and fuel exhaust valves time constants, respectively (s).
ω_e	Electrical angular velocity of the PMSG rotor [rad/s].
ω	Fundamental frequency of output waveform.
$\Delta\omega$	Per unit change in rotor speed.